



Cite this: *J. Mater. Chem. B*, 2016, 4, 1520

A rapid ammonia sensor based on lysine nanogel-sensitized PANI/PAN nanofibers

De-Qun Wu,* Li-Li Wu, Hai-Chun Cui, Hong-Nan Zhang and Jian-Yong Yu

In this paper, L-lysine-based materials which are rich in amino groups were synthesized through a chemical reaction. The polyaniline/polyacrylonitrile (PANI/PAN) thin film and PANI/PAN nanocomposite (NC) thin films doped with L-lysine based materials were obtained by electrospinning and *in situ* polymerization of aniline. The gas sensing properties of the PANI/PAN thin film and PANI/PAN NC thin films doped with L-lysine based materials towards NH₃, ethanol, acetone, chloroform and DMF were examined at room temperature. The experimental results reveal that the PANI/PAN/L-lysine based nanogel (4-Lys-4 nanogel) NC thin film exhibited a highly selective response toward NH₃ at room temperature with improved response kinetics. The PANI/PAN/4-Lys-4 nanogel NC thin film showed the response of 5.5 with response and recovery times of 22 s and 15 s, respectively, toward 100 ppm NH₃, and the detection limit of 2.2 ppm. This response and recovery are quite fast compared with the reported studies based on PANI doped with other materials. The enhanced response could be attributed to the large surface area, the core-shell structure of the nanofibers and improved charge transfer as a result of a certain amount of amino groups doping PANI. Our results clearly indicate that the PANI/PAN/4-Lys-4 nanogel NC thin film could effectively be used for the practical room temperature NH₃ sensing application with quite fast response and recovery properties. At the same time, a new application of 4-Lys-4 nanogel on sensors is supplied.

Received 4th October 2015,
Accepted 26th January 2016

DOI: 10.1039/c5tb02058a

www.rsc.org/MaterialsB

1. Introduction

Ammonia, as a colorless, highly toxic gas, is attracting more and more attention of researchers. Nowadays, more and more ammonia in our atmosphere comes from human activities, such as chemical plants, refrigeration and motor vehicles.¹ If humans are exposed to a high concentration of ammonia, the skin and eyes would be injured. Therefore, finding a fast, convenient and inexpensive technique to detect ammonia in air is critical for environmental monitoring.²

Intrinsic conducting polymers (ICPs) have made a great impact on many different technologies since their discovery. The ICs have a wide range of applications, including junction devices, electromagnetic interference shields, molecular recognition and energy storage.^{3–5} Many researchers have investigated chemical sensors using conducting polymers as sensitive materials due to their selectivity over a wide range of analyte molecules and fast response to certain gas molecules. Polyaniline (PANI), as one of the most promising conducting polymers, has received much attention from researchers⁶ due to its cheap monomers, stability under ambient conditions, easy to synthesize with a high yield

and controllable electrical conductivity.⁷ It has different forms according to its oxidation state, the conductive form of PANI, the protonated polyemeraldine or polyemeraldine salt, whose color is green.⁸ Polyaniline, synthesized from the oxidative polymerization of aniline, whose conductivity can be controlled by protonation/deprotonation in an acid–base chemical interactions.^{3,9,10} Polyaniline in the emeraldine salt form is an ideal sensing layer for the detection of NH₃ because of the similar roles played by the nitrogen atoms of compounds in establishing coordinate bonding with protons on the polymer chains, and the mechanism is illustrated in the literature.⁸ However, the response of the pure PANI to NH₃ is not high and the response and recovery times are quite long. Therefore, some researchers used certain materials doping PANI to improve the sensitivity for NH₃.

Jin *et al.*⁴ have presented an optical ammonia gas sensor based on a PANI film prepared by chemical oxidation, which is sensitive, stable, fast in response, but it is not very easy to recover. Nanocomposite films by incorporating Cu,² CSA,¹¹ graphene,^{12,13} MWCNT,¹⁴ acrylic acid¹⁵ into the PANI matrix have demonstrated better sensitivity to ammonia. For example, Patil *et al.*² reported thin films of the copper nanoparticles intercalated polyaniline nanocomposite, which had higher sensitivity and faster in response compared with pure polyaniline. The response and recovery times of the composite films toward 50 ppm of ammonia were 7 and 160 s, respectively.

Key Laboratory of Textile Science & Technology, Ministry Education, College of Textiles, Donghua University, No. 2999 North Renmin Road, Songjiang, Shanghai, 201620, China. E-mail: dqwu@dhu.edu.cn

Wojkiewicz *et al.*⁹ reported PANI/core-shell structure nanoparticle-based NC thin films that have larger sensitivity than the nanofiber-based one, but their response time is 2.5 minutes to 1 ppm NH₃, which is quite long.

Nanomaterials, such as nanofibers,¹⁶ nanotubes,¹⁷ and nanoribbons,¹⁸ possessing high specific surface areas, which could facilitate fast diffusion of gas molecules into sensitive films.¹⁹ Electrospinning (ES), a technology developed more than 100 years ago, with the feature of ease of fabrication of continuous nanofibers, has received much attention from the people who concerned much about nanostructured materials.²⁰ Herein, L-lysine based materials which are rich in amino groups²¹ were added into the polyacrylonitrile (PAN) electrospinning solutions to form nanofiber films.²² Then PANI was polymerized on the surface of the blended electrospun nanofiber films.²³ The ammonia gas sensing properties of different L-lysine based materials incorporated PANI NC thin films were investigated. Furthermore, the NH₃ sensing properties of the nanogel-doped PANI/PAN NC thin film were reported, which are quite good compared to other three nanofiber films: higher response, shorter response and recovery times. These results show a promising approach in the realization of a high-performance ammonia sensor, at the same time, a new application of L-lysine based nanogel on sensors is supplied.

2. Experimental

2.1 Materials

L-Lysine monohydrochloride (Lys), *p*-toluenesulfonic acid monohydrate (TosOH·H₂O), adipoyl chloride, 1,4-butanediol (Alfa Aesar, Ward Hill, MA), *p*-nitrophenol (J. T. Baker, Phillipsburg, NJ), aniline, ferric chloride hexahydrate (FeCl₃·6H₂O), L-camphorsulfonic acid (L-CSA), ammonia (AR grade), and polyacrylonitrile (PAN, *M_w* = 75 000) were used without further purification. Triethylamine (TEA) obtained from Fisher Scientific (Fairlawn, NJ) was dried *via* refluxing with calcium hydride followed by distillation. Other solvents, such as toluene, ethyl acetate, acetone, isopropanol, *N,N*-dimethylformamide (DMF), *N,N*-dimethylacetamide (DMAc) and dimethyl sulfoxide (DMSO) were purchased from VWR Scientific (West Chester, PA) and were purified using standard methods before use. Trypsin (Type IX-S, from bovine pancreas, lyophilized power, 13 000–20 000 BAEE units per mg protein) was purchased from Pierce (Rockford, IL).

2.2 Synthesis of the Lys-4 monomer and di-*p*-nitrophenyl adipate (NA)

The syntheses of the di-*p*-toluenesulfonic acid salt of the bis-L-lysine ester (Lys-4) and the di-*p*-nitrophenyl adipate (NA) monomers are described in the previous literature studies.^{21,24}

2.3 Fabrication of the lysine based polymer and its macrogel

The Lys-based polymer (4-Lys-4 polymer) and its macrogel (4-Lys-4 macrogel) were prepared by a direct polycondensation reaction of the Lys-4 monomer and the NA monomer at 80 °C in DMAc. The fabrication of 4-Lys-4 macrogel with NA and Lys-4 at a molar

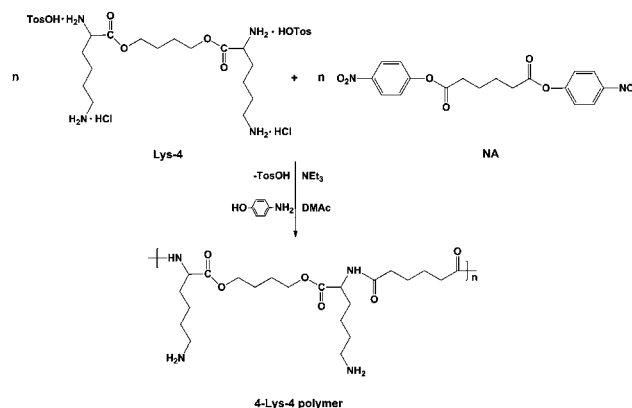


Fig. 1 Illustration of the chemical synthesis of the 4-Lys-4 polymer.

ratio of 1.5 : 1 is described in the previous literature.²¹ In order to obtain the 4-Lys-4 polymer, the NA and Lys-4 monomers at a feed molar ratio of 1 : 1 were added to a vial and dissolved in DMAc at 50 °C under magnetic stirring, and then triethylamine (TEA) (4.5 eq. to Lys-4) was added. The above mixed solution was placed in an 80 °C oil bath for 12 h under stirring. The resulting solution was precipitated with cold ethyl acetate, filtered, extracted by ethyl acetate in a Soxhlet apparatus for 48 h, and at last dried *in vacuo* at 50 °C. The synthesis of the 4-Lys-4 polymer is illustrated in Fig. 1.

2.4 *In vitro* enzymatic biodegradation of 4-Lys-4 macrogel

The biodegradation of 4-Lys-4 macrogel was carried out in a small vial, which contained a small piece of known weight dry macrogel sample (*ca.* 50 mg) and 10 mL of PBS buffer (pH 7.4, 0.1 M) with trypsin at a concentration of 0.1 mg mL⁻¹. The vial was then incubated at 37 °C, the incubation media were refreshed daily in order to maintain the enzymatic activity. At predetermined immersion durations, the macrogel samples were removed from the incubation medium, and then washed three times with PBS. The resultant mixture was dialyzed against distilled water for two days and lyophilized *in vacuo* using a FreeZone Benchtop and Console Freeze Dry System (Model 7750000, LABCONCO Co., Kansas City, MO) at -48 °C for 72 h.

In order to observe the size and morphology of nanogel generated from the biodegradation of macrogel in the enzyme solution at a predetermined time, a few drops of the biodegradation solution were collected for TEM characterization.

2.5 Preparation of PANI/PAN NC thin films doped with L-lysine based materials

Four different electrospinning solutions (3.0 g respectively) were prepared as following: the solutions of 10.0 wt% PAN, 10.0 wt% PAN with 1.0 wt% Lys-4, 10.0 wt% PAN with 1.0 wt% 4-Lys-4 and 10.0 wt% PAN with 1.0 wt% nanogel were prepared in DMF under magnetic stirring at room temperature for 10 h. The 10.0 wt% PAN with 1.0 wt% 4-Lys-4 polymer solution was prepared by mixing two solutions: 0.48 g of 4-Lys-4 polymer solution (6.67 wt%) was prepared in DMSO at room temperature under vigorous stirring for 4 h; 2.52 g of PAN solution

Table 1 Electrospinning solution parameters of four different blending systems

Sample	Solutes	Solvent
1	0.3 g PAN	2.70 g DMF
2	0.3 g PAN + 0.03 g Lys-4	2.67 g DMF
3	0.3 g PAN + 0.03 g 4-Lys-4 polymer	2.225 g DMF + 0.445 g DMSO
4	0.3 g PAN + 0.03 g nanogel	2.67 g DMF

(13.5 wt%) was prepared in DMF at room temperature under vigorous stirring for 10 h. Then the mixed solution was obtained under stirring for 4 h. The detailed information about the electrospinning solutions is listed in Table 1.

The electrospinning solution was loaded into a syringe, which was attached to a high-voltage power supply (EST804A, Shenzhen Huyi Science & Technology Co., Ltd) that was capable of generating voltages up to 50 kV. The applied voltage was set as 10 kV. A syringe pump (LSP01-1A, Baoding Longer Precision Pump Co., Ltd) was used to regulate the flow of the solution. The flow rate was kept at 0.45 mL h^{-1} . An aluminum foil with the dimension of $30 \times 30 \text{ cm}$ was used as the collector, the tip-to-collector distance was 12 cm. The electrospinning chamber was kept at the constant temperature (20°C) and RH (40%). Fibrous membranes were continuously deposited on the aluminum foil. After electrospinning, the nanofiber films were dried *in vacuo* at 80°C for 72 h to remove residual DMF and DMSO. The electrospinning setup used in the experiments is schematically shown in Fig. 2a.

The deposition of conductive polyaniline (polyaniline emeraldine salt) onto the electrospun PAN nanofibers was achieved by *in situ* polymerization. Polyaniline was obtained by the chemical polymerization of aniline using $\text{FeCl}_3 \cdot 6\text{H}_2\text{O}$ as an oxidant²⁵ and *l*-camphorsulfonic acid (*l*-CSA) as the acid dopant. The laboratory procedure was used to produce electrically conducting composite electrospun fiber films in this study, which is shown in Fig. 2b. Typically, $8 \times 10^{-3} \text{ mol}$ aniline and $8 \times 10^{-3} \text{ mol}$ *l*-CSA were mixed in 40 mL of distilled water. Before oxidative polymerization, the solution was cooled in an ice bath ($0\text{--}5^\circ\text{C}$). At the same time, four different nanofiber films ($3 \text{ cm} \times 3 \text{ cm}$) were detached from aluminum foils and immersed in an aqueous solution of $\text{FeCl}_3 \cdot 6\text{H}_2\text{O}$ ($4 \times 10^{-3} \text{ mol}$ in 10 mL of distilled water) for 10 minutes, respectively. Then, 10 mL of the cooled mixture solution was added to the aqueous solution of $\text{FeCl}_3 \cdot 6\text{H}_2\text{O}$, respectively, and reacted in the ice bath for 2 h. The reaction mixtures were shaken gently, and the PANI layer formed gradually on the surface of the nanofibers. After the nanofiber films were removed from the reaction mixture, they were rinsed with distilled water to remove the reactant and excess PANI that precipitated on the nanofiber films surface.

2.6 Characterization

The surface morphology of the films was studied using field emission scanning electron microscope (FE-SEM, S-4800). The structure of the core-shell nanofibers was characterized by transmission electron microscopy (TEM, JEM-2100). Fourier-transform infrared (FT-IR, Nicolet 6700) spectroscopy of five

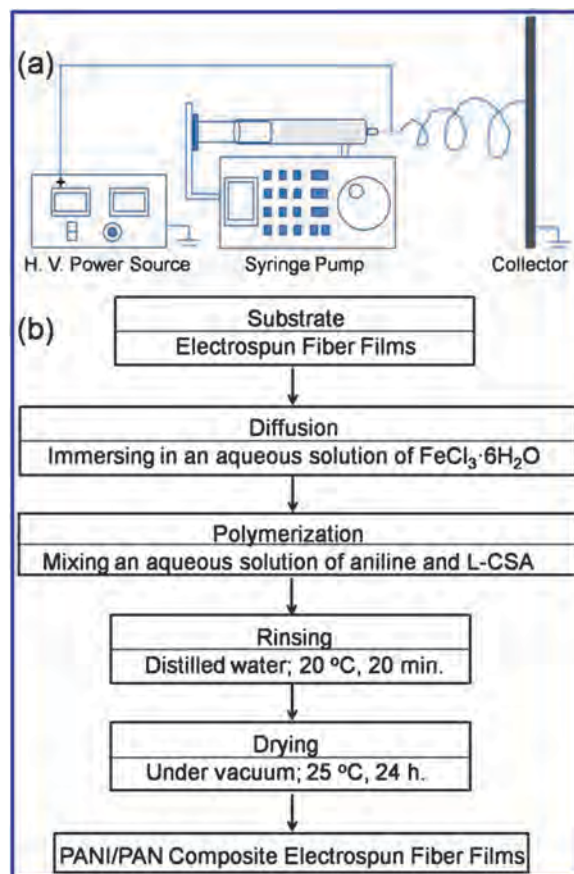


Fig. 2 (a) Schematic representation of the electrospinning system. (b) Schematic diagram of the PANI/PAN composite films preparation process.

different chemical structures of the films was characterized. The size and size distribution of the 4-Lys-4 nanogel was determined using a particle size and zeta potential analyzer (Nano ZS, Malvern Instruments). The aqueous solution (200 mg L^{-1}) containing nanogel was passed through a $0.45 \mu\text{m}$ pore size filter prior to measurement.

2.7 Gas sensing measurements

The gas sensing properties of the sensor were measured using a CGS-1TP (Chemical Gas Sensor-1 Temperature Pressure) intelligent gas sensing analysis system (Beijing Elite Tech Co. Ltd, China), which was reported to be used by Feng *et al.*²⁶ and Zhang *et al.*²⁷ This multifunctional system consisted of the heating system, gas distribution system, probe adjustment system, vacuum system, measurement and data acquisition system, and measurement control software. The analysis system offered an external temperature control (from room temperature to 500°C), which could adjust the sensor temperature directly. The sensor substrates ($13.5 \text{ mm} \times 7 \text{ mm}$, 0.5 mm in thickness) with Ag-Pd interdigitated electrodes (both the width and the distance were $200 \mu\text{m}$) were purchased from Beijing Elite Tech Co., Ltd.

Four different fibrous membranes ($5 \text{ mm} \times 3 \text{ mm}$) were spread on the sensor substrates respectively. Two probes were

pressed on sensor substrates to export electrical signals. When the resistance of the sensor was stable, the saturated target gas solution was injected into the test chamber (18 L in volume) using a micro-injector through a rubber plug with the evaporation temperature of 80 °C. The target gas was mixed with air (relative humidity was about 50%) by two fans in the analysis system. The test chamber was opened to recover the sensor in air after the sensor resistance reached a new constant value. The sensor resistance and sensitivity were collected by the system in real time.

The sensitivity of the sensor was characterized by the response value (R): the higher R , the better sensitivity. R was designated as $R = R_g/R_a$, where R_a is the sensor resistance in air (base resistance) and R_g is sensor resistance in a mixture of target gas and air. The time taken by the sensor resistance to change from R_a to $R_a + 90\% \times (R_g - R_a)$ was defined as the response time when the target gas was introduced into the sensor, and the time taken from R_g to $R_g - 90\% \times (R_g - R_a)$ was defined as the recovery time when the ambience was replaced by air. All sensing experiments were carried out at room temperature (25 °C).

3. Results and discussion

3.1 Synthesis of the monomers, polymer and hydrogel

The lysine-based polymer and its macrogel were polymerized from the Lys-4 monomer and NA *via* a simple polycondensation reaction. The ^1H NMR spectrum of the Lys-4 monomer and the 4-Lys-4 polymer are illustrated in Fig. 3a. As shown in Fig. 3a(A), the chemical shift δ at 7.75 and 7.14 ppm (the phenyl group of TosOH attached to the amine group, (c and b)), δ at 4.15 ppm ((e) $-\text{C}=\text{O}-\text{O}-\text{CH}_2-$), δ at 3.45 ppm ((d) $-\text{C}=\text{O}-\text{O}-\text{CH}-\text{NH}_2$), δ at 2.80 ppm ((g) $-\text{CH}_2-\text{NH}_2$), δ at 2.34 ppm ((a) phenyl- CH_3), δ at 1.90 ppm ((h) $-\text{CH}-\text{CH}_2-\text{CH}_2-$), δ at 1.62 ppm ((f) $-\text{CH}_2-\text{CH}_2-\text{CH}_2-$), δ at 1.45 ppm ((j) $-\text{CH}_2-\text{CH}_2-\text{CH}_2-$) and δ at 1.12 ppm ((i) $-\text{CH}_2-\text{CH}_2-\text{CH}_2-$). Fig. 3a(B) shows the ^1H NMR spectrum of the 4-Lys-4 polymer. The chemical shift δ at 8.03 ppm ((h) $-\text{C}=\text{O}-\text{NH}-$), δ at 5.11 ppm ((g) $-\text{CH}_2-\text{NH}_2$), δ at 4.08 ppm ((f) $-\text{C}=\text{O}-\text{O}-\text{CH}_2-$), δ at 3.45 ppm ((a) $-\text{C}=\text{O}-\text{O}-\text{CH}-\text{NH}-$), δ at 2.78 ppm ((e) $-\text{CH}_2-\text{NH}_2$), δ at 2.25 ppm ((k) $-\text{CH}_2-\text{CH}_2-\text{C}=\text{O}-$), δ at 2.05 ppm ((i) $-\text{C}=\text{O}-\text{CH}_2-\text{CH}_2-$), δ at 1.75 ppm ((b) $-\text{CH}-\text{CH}_2-\text{CH}_2-$), δ at 1.58 ppm ((l) $-\text{CH}_2-\text{CH}_2-\text{CH}_2-$), δ at 1.47 ppm ((d) $-\text{CH}_2-\text{CH}_2-\text{CH}_2-$) and δ at 1.25 ppm ((c) $-\text{CH}_2-\text{CH}_2-\text{CH}_2-$). According to the monomer ratio, the final polymerized products could be polymers or crosslinked polymers (macrogels). The three dimensional structure of the macrogel is directly determined or related to the intrinsic chemical structure of the macro hydrogel,²⁸ which is one of the most important factors to obtain nanogels *via* an enzyme biodegradation strategy. Before the biodegradation study, the surface morphology of the macrogel was characterized by its optical image, the interior morphology of the freeze-dried 4-Lys-4 macrogel was characterized by SEM. Because of the general degradation capability of the trypsin, it is used as a model enzyme. The hydrogel was biodegraded using 0.1 mg mL⁻¹ of trypsin PBS solution. After 7 days of

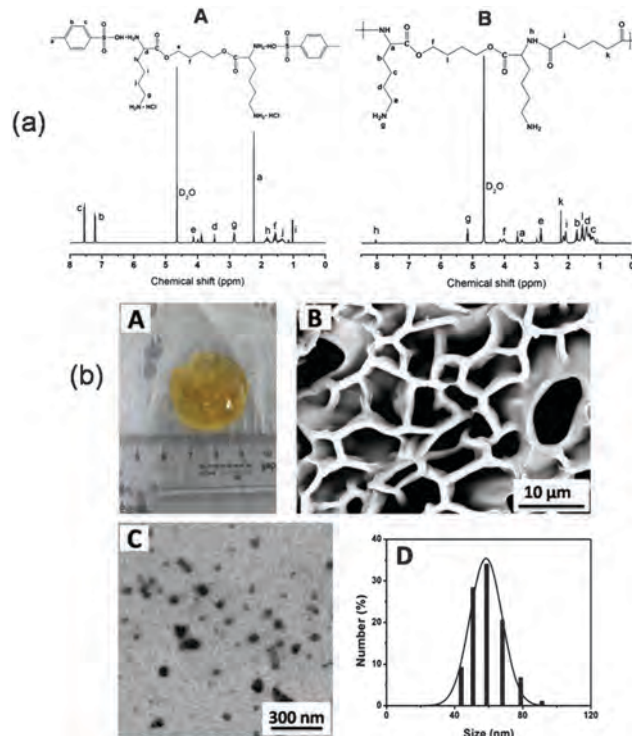


Fig. 3 (a) ^1H NMR spectrum of (A) the Lys-4 monomer and (B) the 4-Lys-4 polymer (300 MHz, D_2O). (b) (A) Optical image of the hydrogel; (B) the SEM image of the hydrogel before degradation; (C) the TEM image of the macrogel at an enzyme trypsin concentration of 0.1 mg mL⁻¹ in PBS buffer (pH 7.4, 0.1 M) after 7 days of biodegradation; (D) DLS of the 7 day biodegradation of macrogel.

biodegradation,²⁹ the nanogels were collected and characterized using TEM and particle size and zeta potential analyzer. The enzyme trypsin was removed by dialysis (cutoff weight 100 000). As shown in Fig. 3b, before biodegradation, the hydrogel exhibited well-defined, three dimensional porous and completely connected network structures with an average wall thickness of about 1.2–1.8 μm and an average pore size of around 2.0–8.0 μm . After 7 days biodegradation, the size of the obtained nanogels was about 60 nm with a narrow size distribution.

3.2 Characterization of PANI/PAN coaxial nanofibers

In this study, PANI/PAN coaxial nanofibers doped with Lys-4 and 4-Lys-4 polymers, and 4-Lys-4 nanogel were prepared by a combination of an electrospinning technique and an *in situ* polymerization method respectively. The SEM and TEM images of the nanofibers of PAN and its composite with PANI are shown in Fig. 4. It can be seen clearly that the nanofibers electrospun from PAN in DMF solution with a weight percentage of 10.0 had a diameter of about 200 nm. After the deposition of PANI by *in situ* polymerization, the diameters of the fibers were increased to 250–300 nm in average. It is obviously observed that the core-shell structure of the composite nanofibers is shown in Fig. 4D, the surface of the composite nanofibers was much rougher than that of PAN nanofibers, which increased the specific surface area of the sensitive membrane. The thickness of PANI is about

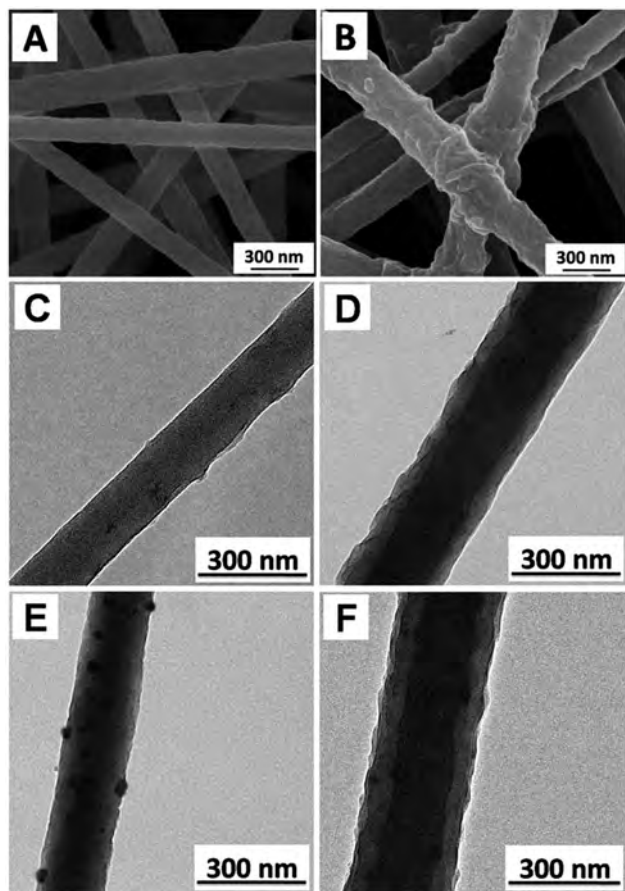


Fig. 4 SEM images of (A) PAN nanofibers and (B) PANI/PAN coaxial nanofibers, TEM images of (C) PAN nanofibers, (D) PANI/PAN coaxial nanofibers, (E) PAN/4-Lys-4 nanogel nanofibers and (F) PANI/PAN/4-Lys-4 nanogel coaxial nanofibers.

50 nm as shown in Fig. 4D. As shown in Fig. 4E, 4-Lys-4 nanogels were electrospun into PAN nanofibers, which are embedded easily in the surface of the electrospinning nanofibers.

3.3 FT-IR spectra of PAN and PANI/PAN composite thin films

Fig. 5 shows the FT-IR spectra recorded in the spectral range of 800–3600 cm^{-1} of five different electrospinning thin films. The peak at 2242 cm^{-1} is assigned to the stretching vibration of nitrile groups ($-\text{CN}-$).³⁰ The presence of the peak at 2934 cm^{-1} can be attributed to the C–H stretching vibrations of PAN. The bands appearing at wavenumbers 1589 and 1453 cm^{-1} correspond to the C=N (Fig. 5V) and C=C (Fig. 5IV)³¹ stretching modes attributed to the quinoid and benzenoid rings, respectively. As shown in Fig. 5, only the pure PAN electrospinning thin film don't have these two bands, which confirms that PANI have deposited on the other four electrospinning thin films. The band characteristic of the conducting protonated form is observed at 1250 cm^{-1} and interpreted as a C–N⁺ (Fig. 5III) stretching vibration in the polaron structure. The main peaks at 1171 cm^{-1} in the spectrum of these four films correspond to a vibration mode of the $-\text{NH}^+=$ (Fig. 5II) structure,³² which occurs due to the protonation of PANI. The band at 1039 cm^{-1} due to

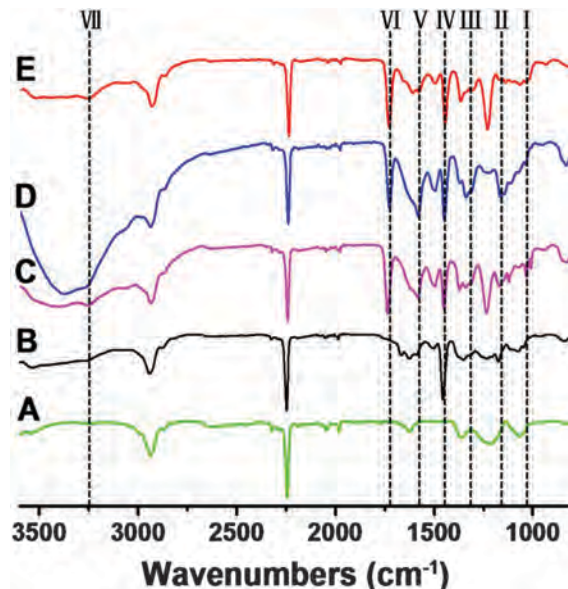


Fig. 5 FT-IR spectra of five different electrospinning thin films: (A) PAN; (B) PANI/PAN; (C) PANI/PAN/Lys-4; (D) PANI/PAN/4-Lys-4 polymer; (E) PANI/PAN/4-Lys-4 nanogel.

the S=O (Fig. 5I) stretching confirms the presence of sulfonic groups in the L-CSA.¹¹ The characteristic bands at 1742 and 3263 cm^{-1} in the spectrum of NC thin films of PANI/PAN/Lys-4, the PANI/PAN/4-Lys-4 polymer and PANI/PAN/4-Lys-4 nanogel are attributed to the C=O (Fig. 5VI) stretching and N–H (Fig. 5VII) stretching of aromatic amines,³³ which confirms that the lysine based materials have doped in the PANI/PAN NC thin films.

3.4 Evaluation of gas-sensing performance

It is well known that response and recovery characterization are important for evaluating the performances of ammonia sensors. Fig. 6a shows the response curves of four different PANI/PAN NC thin films upon exposure to different concentrations of NH_3 ranging from 5 to 2000 ppm at room temperature. It can be easily found that the response increased rapidly with the increase of the ammonia concentration (5–300 ppm), and then gradually slowed down (300–2000 ppm), which indicated that the sensor films become saturated gradually. Finally, the films reached saturation at about 2000 ppm. It is also

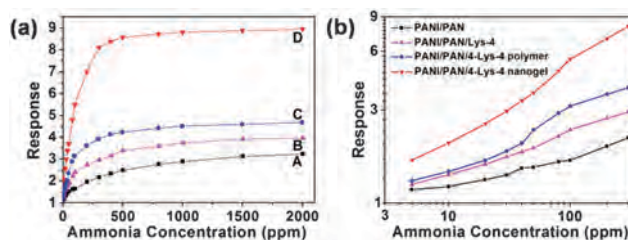


Fig. 6 (a) The response of four different PANI/PAN NC thin films versus ammonia concentrations. (A) PANI/PAN; (B) PANI/PAN/Lys-4; (C) PANI/PAN/4-Lys-4 polymer; (D) PANI/PAN/4-Lys-4 nanogel. (b) Dependence of response of four different PANI/PAN NC thin films on ammonia concentration of 5 to 300 ppm at room temperature.

Table 2 The detection limit, response and recovery times of four different NC thin films

NC thin film	I	II	III	IV
Detection limit (ppm)	6.5	3.7	3.5	2.2
Response time (s)	56	30	33	22
Recovery time (s)	58	24	34	15

I: PANI/PAN; II: PANI/PAN/Lys-4; III: PANI/PAN/4-Lys-4 polymer; IV: PANI/PAN/4-Lys-4 nanogel.

demonstrated that the response of the pure PANI/PAN NC thin film, the PANI/PAN NC thin film doped with the Lys-4 and 4-Lys-4 polymers, and 4-Lys-4 nanogel increased in varying degrees. The response to 500 ppm ammonia reaches 8.546 when the film doped with nanogel was used, while that value is only 2.484 when the pure PANI/PAN film was tested. While the response of the PANI/PAN NC thin films doped with the Lys-4 and 4-Lys-4 polymers are 3.374 and 4.234, respectively.

Dependence of response of four different PANI/PAN NC thin films on ammonia concentration of 5 to 300 ppm was shown in Fig. 6b. The detection limit is defined as the concentration at which response is 1.1, corresponding to 10% change of resistance. The detection limits of four different NC thin films are listed in Table 2. Compared to other three NC thin films, the detection limit of the NC thin film of PANI/PAN/4-Lys-4 nanogel was much lower, *i.e.*, 2.2 ppm.

There are several reasons which should be considered to explain the improvement of the nanofibers' sensing performance upon lysine-based materials doping. To describe the sensitization mechanism more clearly, we present a simple model in Fig. 7. As shown in the scheme, the whole process can be divided into three steps. As supposed, step 1 is the synthesis of PANI on the surface of PAN nanofibers (Fig. 7a). In this step, $-\text{NH}_2$ and $-\text{N}=\text{}$ were converted into $-\text{NH}_3^+$ and $-\text{NH}^+=$, respectively, because of L-CSA, which is vital to the sensing process for NH_3 . Step 2 is the process of NH_3 contacted with the surface of the NC fibers (Fig. 7b). NH_3 reacted with $-\text{NH}^+=$ to form $-\text{N}=\text{}$, then H^+ of the $-\text{NH}_3^+$ transferred to $-\text{N}=\text{}$. Then NH_3 reacted with the new formed $-\text{NH}^+=$ to form $-\text{N}=\text{}$, which is defined as step 3 (Fig. 7c). The whole process achieved the change of the resistance of sensitive NC fibers. Therefore, with the amino groups doping in the PANI/PAN nanofibers, the response is higher than that of the pure PANI/PAN nanofibers, the response and recovery times are shorter as well. When the ammonia environment disappears, the sensitive NC fibers' resistance will back to the original state. This would be explained in the following section.

Because the number of amino groups and the forms of Lys-4, 4-Lys-4 polymer and 4-Lys-4 nanogel are different, the sensitivity of the three NC thin films to ammonia is different. Lys-4 and 4-Lys-4 polymers are powder, which could dissolve in the solvent homogeneously and form uniform nanofibers by electrospinning. However, 4-Lys-4 nanogels are granular, which are easier in the surface of the electrospinning nanofibers. In addition, the amino groups of Lys-4 are protected by hydrochloric acid and *p*-toluenesulfonic acid even though the number of amino groups of Lys-4 is more than that of the 4-Lys-4 polymer. Therefore, the

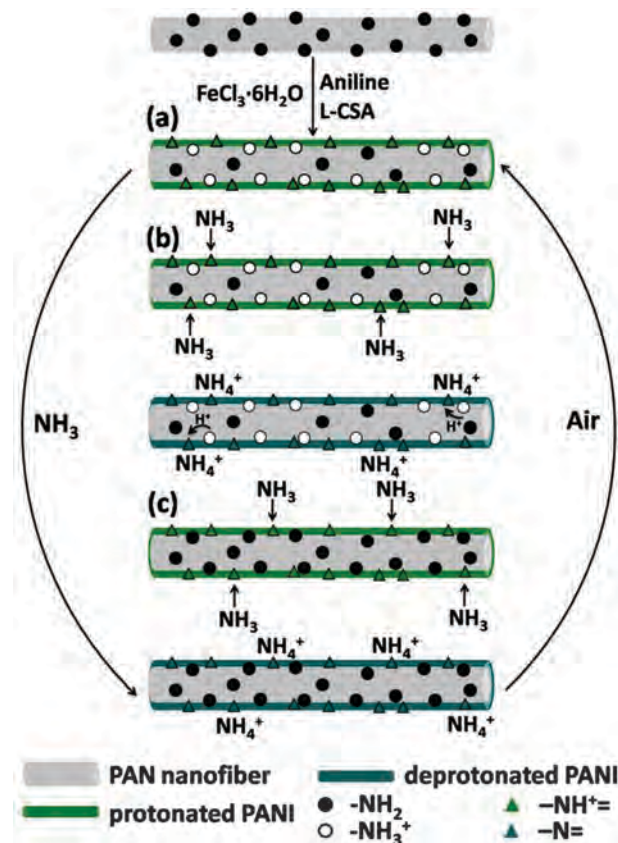
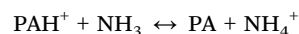


Fig. 7 Schematic model of the three steps for the sensitization mechanism of the prepared nanofiber sensor: (a) PANI was synthesized on the surface of PAN nanofibers, at the same time, $-\text{NH}_2$ and $-\text{N}=\text{}$ were converted into $-\text{NH}_3^+$ and $-\text{NH}^+=$, respectively, because of L-CSA; (b) NH_3 contacted with the surface of the NC fibers, NH_3 reacted with $-\text{NH}^+=$ to form $-\text{N}=\text{}$, then H^+ of the $-\text{NH}_3^+$ transferred to $-\text{N}=\text{}$; (c) NH_3 reacted with the new formed $-\text{NH}^+=$.

sensitivity, the response and recovery properties of the PANI/PAN/4-Lys-4 nanogel thin film are the best.

The resistance of the films is found to increase when exposed to NH_3 ambient and decrease when exposed to air (as shown in Fig. 8), which is due to the fact that the electrons of NH_3 act as the donor to the p-type PANI, thus causing a reduction of hole concentration in the PANI, *i.e.*, the deprotonation reaction causes the resistance of the PANI layer to grow.^{15,34} The sensing mechanism can be explained as follows. When the PANI/PAN NC thin films exposed to ammonia, the following reversible reaction occurs:



where PA and PAH^+ are the initial undoped repeated block and the proton-doped repeated block of the PANI chains, respectively.

In the presence of ammonia, this reaction goes predominantly towards the right, the protonated PANI loses protons and ammonia reacts with the protons producing energetically more favourable ammonium ions. But in air the reaction begins to go towards the left, ammonium ion decomposes into ammonia and protons, which were added to the PANI molecules, make the film regain its initial level of doping.

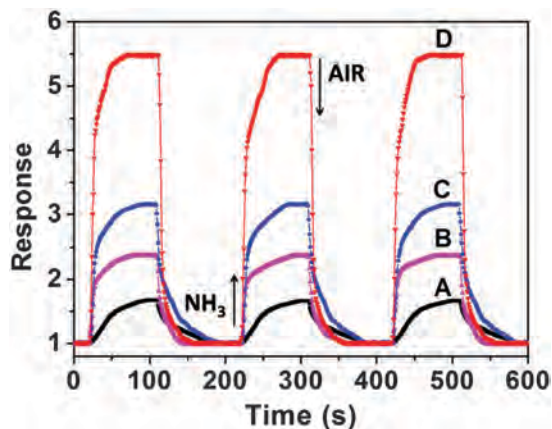


Fig. 8 Response and recovery behaviors of four different PANI/PAN NC thin films to 100 ppm ammonia at room temperature. (A) PANI/PAN; (B) PANI/PAN/Lys-4; (C) PANI/PAN/4-Lys-4 polymer; (D) PANI/PAN/4-Lys-4 nanogel.

Fig. 8 shows the response–recovery characteristic of four different PANI/PAN NC thin films exposed to 100 ppm ammonia at room temperature. When ammonia was injected into the testing chamber, the responses of four different sensors increased rapidly; when subjected to air, the sensor recovery to the initial state was also rapid, the response and recovery times were less than one minute. The detailed information about the response and recovery time of four different NC thin films is listed in Table 2. Compared to other three NC thin films, the response and recovery times of the PANI/PAN NC thin film doped with nanogel were much shorter, *i.e.*, 22 s and 15 s, respectively. The rapid response and recovery of the sensors can be attributed to the 1D nanostructure of electrospun nanofibers, which can facilitate fast mass transfer of ammonia molecules to the interaction region as well as improve the rate for charge carriers to traverse the barriers introduced by molecular recognition events along the entire fibers. Moreover, the surface of the NC thin film doped with nanogel is much rougher because of the nanogel, which increases the effective specific surface area of the sensitivity film. Therefore, its response and recovery are quicker than that of other films.

The NH_3 gas sensing properties of PANI/PAN/4-Lys-4 nanogels and other conducting polymer materials in the reported literature are compared, as shown in Table 3. It can be seen that the sensor based on the PANI/PAN/4-Lys-4 nanogel thin film has good performance for the ammonia gas detection. Its response and recovery times are much shorter, 22 s and 15 s, to 100 ppm NH_3 , respectively. Even though some materials, such as MWNTs/33 wt% PANI, 0.13 at% Cu/PANI, hexagonal structures CSA/PANI, response to NH_3 very fast, the recovery times are more than 2 minutes. These results suggest that the PANI/PAN/4-Lys-4 nanogel thin film has not only the shorter response time but also the shorter recovery time compared with other conducting polymer materials.

The good selectivity is also a very important factor to a gas sensor when it detects the target gas in the presence of many different gases. To evaluate the selectivity of the sensor, other gases are used as the target gas. As shown in Fig. 9, they are the responses of four PANI/PAN NC thin films to 100 ppm

Table 3 Metrological parameters for the nanostructured sensor materials

Sensing material	Concentration of NH_3 (ppm)	Response time	Recovery time	Measured temperature ($^{\circ}\text{C}$)	Ref.
I	100	22 s	15 s	25	This paper
II	100	21 s	> 202 s	R.T.	14
III	1250	2.27 min	9.73 min	26	35
IV	50	7 s	160 s	R.T.	2
V	20	60–100 s	1–5 min	R.T.	34
VI	200	1 s	~ 7 min	R.T.	11
VII	80	> 2.5 min	> 10 min	25	9
VIII	100	50 s	23 s	25	12

Materials I: PANI/PAN/4-Lys-4 nanogel; II: MWNTs/33 wt% PANI; III: tapered multimode fiber/PANI; IV: 0.13 at% Cu/PANI; V: silicon with SAM/PANI; VI: hexagonal structures CSA/PANI; VII: PU–PANI nanorods (CSA); VIII: graphene/PANI. R.T.: room temperature.

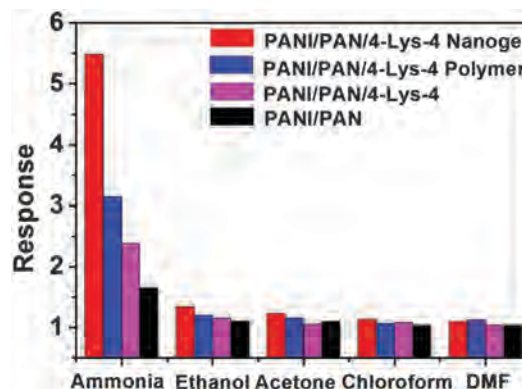


Fig. 9 Responses of four PANI/PAN NC thin films to different gases (100 ppm) at room temperature.

ammonia, ethanol, acetone, chloroform, DMF at room temperature. It shows that the four PANI/PAN NC thin films have higher response to ammonia compared with that to the other four gases. This confirms that all the four NC thin films have selectivity to ammonia. As for the four PANI/PAN NC thin films, their responses to ammonia have a big difference, whereas their responses to ethanol, acetone, chloroform and DMF only have a little difference. The response of the PANI/PAN/4-Lys-4 nanogel thin film to ammonia is much higher than that of other three NC thin films; therefore, the PANI/PAN/4-Lys-4 nanogel thin film have the best selectivity to ammonia, *i.e.*, the PANI/PAN/4-Lys-4 nanogel thin film has a great potential to be a sensor for highly selective detection of ammonia.

Conclusions

In conclusion, the PANI/PAN thin film and PANI/PAN NC thin films doped with L-lysine based materials were obtained by electrospinning and *in situ* polymerization of aniline. The gas sensing properties of the PANI/PAN thin film and PANI/PAN NC thin films doped with L-lysine based materials towards NH_3 , ethanol, acetone, chloroform and DMF were examined at room temperature. The experimental results reveal that the

PANI/PAN/4-Lys-4 nanogel NC thin film exhibited a highly selective response toward NH_3 at room temperature with improved response kinetics. The PANI/PAN/4-Lys-4 nanogel NC thin film showed the response of 5.5 with the response and recovery times of 22 s and 15 s, respectively, toward 100 ppm NH_3 , its detection limit could be 2.2 ppm. This response and recovery are quite fast compared with the reported studies based on PANI doped with other materials. The enhanced response could be attributed to the large surface area, the core-shell structure of the nanofibers and improved charge transfer as a result of a certain amount of amino groups doping PANI. Our results clearly indicate that the PANI/PAN/4-Lys-4 nanogel NC thin film could effectively be used for the practical room temperature NH_3 sensing application with quite fast response and recovery properties.

Acknowledgements

The research was supported by the Fundamental Research Funds for the Central Universities and sponsored by the Shanghai Pujiang Program 14PJ1400300.

Notes and references

- 1 B. Timmer, W. Olthuis and A. van den Berg, *Sens. Actuators, B*, 2005, **107**, 666–677.
- 2 U. V. Patil, N. S. Ramgir, N. Karmakar, A. Bhogale, A. K. Debnath, D. K. Aswal, S. K. Gupta and D. C. Kothari, *Appl. Surf. Sci.*, 2015, **339**, 69–74.
- 3 S. K. Dhawan, D. Kumar, M. K. Ram, S. Chandra and D. C. Trivedi, *Sens. Actuators, B*, 1997, **40**, 99–103.
- 4 J. Zhe, S. Yongxuan and D. Yixiang, *Sens. Actuators, B*, 2001, **B72**, 75–79.
- 5 H. Bai, K. Sheng, P. Zhang, C. Li and G. Shi, *J. Mater. Chem.*, 2011, **21**, 18653–18658.
- 6 A. L. Kukla, Y. M. Shirshov and S. A. Piletsky, *Sens. Actuators, B*, 1996, **37**, 135–140.
- 7 A. Attout, S. Yunus and P. Bertrand, *Polym. Eng. Sci.*, 2008, **48**, 1661–1666.
- 8 D. Nicolas-Debarnot and F. Poncin-Epaillard, *Anal. Chim. Acta*, 2003, **475**, 1–15.
- 9 J. L. Wojkiewicz, V. N. Bliznyuk, S. Carquigny, N. Elkamchi, N. Redon, T. Lasri, A. A. Pud and S. Reynaud, *Sens. Actuators, B*, 2011, **160**, 1394–1403.
- 10 A. Riede, M. Helmstedt, I. Sapurina and J. Stejskal, *J. Colloid Interface Sci.*, 2002, **248**, 413–418.
- 11 D. Verma and V. Dutta, *Sens. Actuators, B*, 2008, **134**, 373–376.
- 12 Z. Wu, X. Chen, S. Zhu, Z. Zhou, Y. Yao, W. Quan and B. Liu, *Sens. Actuators, B*, 2013, **178**, 485–493.
- 13 X. Huang, N. Hu, R. Gao, Y. Yu, Y. Wang, Z. Yang, E. S.-W. Kong, H. Wei and Y. Zhang, *J. Mater. Chem.*, 2012, **22**, 22488–22495.
- 14 L. He, Y. Jia, F. Meng, M. Li and J. Liu, *Mater. Sci. Eng., B*, 2009, **163**, 76–81.
- 15 V. V. Chabukswar, S. Pethkar and A. A. Athawale, *Sens. Actuators, B*, 2001, **77**, 657–663.
- 16 H. Zhang, Z. Li, L. Liu, X. Xu, Z. Wang, W. Wang, W. Zheng, B. Dong and C. Wang, *Sens. Actuators, B*, 2010, **147**, 111–115.
- 17 L. Zhang and M. Wan, *Thin Solid Films*, 2005, **477**, 24–31.
- 18 Z. Li, Y. Fan and J. Zhan, *Eur. J. Inorg. Chem.*, 2010, 3348–3353.
- 19 W. Xianfeng, D. Bin, S. Min, Y. Jianyong and S. Gang, *Sens. Actuators, B*, 2010, **144**, 11–17.
- 20 J. Shanzuo, L. Yang and Y. Mujie, *Sens. Actuators, B*, 2008, **133**, 644–649.
- 21 D.-Q. Wu, J. Wu, X.-H. Qin and C.-C. Chu, *J. Mater. Chem. B*, 2015, **3**, 2286–2294.
- 22 S. F. Fennessey and R. J. Farris, *Polymer*, 2004, **45**, 4217–4225.
- 23 H. Kyung Hwa, O. Kyung Wha and K. Tae Jin, *J. Appl. Polym. Sci.*, 2005, **96**, 983–991.
- 24 K. Guo, C. C. Chu, E. Chkhaidze and R. Katsarava, *J. Polym. Sci., Part A: Polym. Chem.*, 2005, **43**, 1463–1477.
- 25 O. Yavuz, M. K. Ram, M. Aldissi, P. Poddar and S. Hariharan, *J. Mater. Chem.*, 2005, **15**, 810–817.
- 26 C. Feng, W. Li, C. Li, L. Zhu, H. Zhang, Y. Zhang, S. Ruan, W. Chen and L. Yu, *Sens. Actuators, B*, 2012, **166–167**, 83–88.
- 27 X.-J. Zhang and G.-J. Qiao, *Appl. Surf. Sci.*, 2012, **258**, 6643–6647.
- 28 J. Wu, X. Zhao, D. Wu and C. C. Chu, *J. Mater. Chem. B*, 2014, **2**, 6660–6668.
- 29 V. X. Truong, I. A. Barker, M. Tan, L. Mespouille, P. Dubois and A. P. Dove, *J. Mater. Chem. B*, 2013, **1**, 221–229.
- 30 D. Zhang, A. B. Karki, D. Rutman, D. R. Young, A. Wang, D. Cocke, T. H. Ho and Z. Guo, *Polymer*, 2009, **50**, 4189–4198.
- 31 Y. S. Yang and M. X. Wan, *J. Mater. Chem.*, 2002, **12**, 897–901.
- 32 M. Trchova, I. Sedenkova, E. Tobolkova and J. Stejskal, *Polym. Degrad. Stab.*, 2004, **86**, 179–185.
- 33 S. G. Pawar, M. A. Chougule, S. Sen and V. B. Patil, *J. Appl. Polym. Sci.*, 2012, **125**, 1418–1424.
- 34 D. S. Sutar, N. Padma, D. K. Aswal, S. K. Deshpande, S. K. Gupta and J. V. Yakhmi, *Sens. Actuators, B*, 2007, **128**, 286–292.
- 35 S. A. Ibrahim, N. A. Rahman, M. H. Abu Bakar, S. H. Girei, M. H. Yaacob, H. Ahmad and M. A. Mahdi, *Opt. Express*, 2015, **23**, 2837–2845.